Is the QGP formed at RHIC ? A perspective from the BRAHMS experiment.

J. J. Gaardhøje[7] for the BRAHMS Collaboration

I. Arsene[10],I. G. Bearden[7], D. Beavis[1], C. Besliu[10], B. Budick[6], H. Bøggild[7], C. Chasman[1], C. H. Christensen[7], P. Christiansen[7], J. Cibor[3], R. Debbe[1], E. Enger[12], J. J. Gaardhøje[7], M. Germinario[7], K. Hagel[8], O. Hansen[7], A. Holm[7], H. Ito[1,11], A. Jipa[10], F. Jundt[2], J. I. Jørdre[9], C. E. Jørgensen[7], R. Karabowicz[4], E. J. Kim[1], T. Kozik[4], T. M. Larsen[12], J. H. Lee[1], Y. K. Lee[5], S. Lindal[12], R. Lystad[9], G. Løvhøiden[12], Z. Majka[4], A. Makeev[8], B. McBreen[1], M. Mikelsen[12], M. Murray[8,11], J. Natowitz[8], B. Neumann[11], B. S. Nielsen[7], J. Norris[11], D. Ouerdane[7], R. Płaneta[4], F. Rami[2], C. Ristea[10], O. Ristea[10], D. Röhrich[9], B. H. Samset[12], D. Sandberg[7], S. J. Sanders[11], R. A. Scheetz[1], P. Staszel[7,4], T. S. Tveter[12], F. Videbæk[1], R. Wada[8], Z. Yin[9], I. S. Zgura[10]

[1] Brookhaven National Laboratory, Upton, New York 11973, USA
[2] Institut de Recherches Subatomiques and Université Louis Pasteur, Strasbourg, France
[3] Institute of Nuclear Physics, Krakow, Poland
[4] M. Smoluchkowski Inst. of Physics, Jagiellonian University, Krakow, Poland
[5] Johns Hopkins University, Baltimore 21218, USA
[6] New York University, New York 10003, USA
[7] Niels Bohr Institute, University of Copenhagen, Copenhagen 2100, Denmark
[8] Texas A&M University, College Station, Texas, 17843, USA
[9] University of Bergen, Department of Physics, Bergen, Norway
[10] University of Bucharest, Romania
[11] University of Kansas, Lawrence, Kansas 66045, USA
[12] University of Oslo, Department of Physics, Oslo, Norway

We review the main results obtained by the BRAHMS collaboration on the properties of hot and dense nuclear matter produced in ultrarelativistic heavy ion collisions at RHIC. A particular focus of this article, (or white paper), is to try to ascertain to what extent the results collected so far by BRAHMS and by the other 3 experiments operating at RHIC can be taken as evidence for the formation of a state of deconfined partonic matter, the so called quark-gluon-plasma (QGP).

1. Introduction

From the onset of the formulation of the quark model and the first understanding of the nature of the binding and confining potential between quarks almost 35 years ago it has been conjectured that a state of matter characterized by a large density quarks and gluons (under one called partons) might be created for a fleeting moment in violent

nuclear collisions (?, ref. Feynman, Shuryak). This dense state would be characterized by a strongly reduced interaction between its constituents, the partons, such that the partons would exist in a nearly free state. Aptly, the proposed state of matter has been coined the quark gluon plasma (QGP). It now generally thought that the early universe was in a QGP state until its energy density had decreased suffciently , as a result of the adiabatic expansion of the universe, that it could make the transition to ordinary (confined) matter.

Experimental attempts to create the QGP and measure the critical temperature have been going on for more than 20 years, colliding the heaviest nuclei (e.g. Au, Pb or U) and analyzing the fragments and produced particles emanating from such collisions. Center of mass energies per pair of colliding nucleons have risen steadily from the $\sqrt{s_{NN}} \approx 1$ GeV domain of the Bevalac at LBNL, to energies of $\sqrt{s_{NN}} = 5$ GeV at the AGS at BNL, and of $\sqrt{s_{NN}} = 17$ GeV at the SPS accelerator at CERN. No decisive proof of QGP formation was found in these experiments, although a number of signals suggesting the formation of a 'very dense state of matter' were found at SPS (ref. xxx).

With the Relativistic Heavy Ion Collider, RHIC, at Brookhaven National Laboratory a new chapter in the story of the production and study of nuclear matter at extreme energy density and temperature has begun. In collisions between gold nuclei at 100AGeV+100AGeV at RHIC the total energy in the center of mass is almost 40TeV, the largest so far achieved in nucleus-nucleus collisions under laboratory conditions. This energy is so large that, if a sizeable fraction of the initial kinetic energy can be converted into matter production, many thousands of particles can be created in a limited volume, leading to unprecedented large energy densities and thus ideal conditions for the formation of the quark gluon plasma.

RHIC started regular beam operations in the summer of year 2000 with a short commissioning run colliding Au nuclei at $\sqrt{s_{NN}} = 130$ GeV). The first full run at top energy ($\sqrt{s_{NN}} = 200$ GeV) took place in the fall/winter of 2001/2002. The third RHIC run during the winter/spring of 2003 focussed on d+Au and p+p reactions. Recently in 2004, a long high luminosity Au+Au run at $\sqrt{s_{NN}} = 200$ GeV and a short run at ($\sqrt{s_{NN}} = 63$ GeV) have been completed. The collected data are currently being analyzed and only a few very preliminary sample results are available.

The main aim here is to review the available information obtained from these first experiments with the purpose of determining what the experimental results, accumulated so far, allow us to say about the high density state of matter that is created at RHIC in collisions between heavy atomic nuclei.

We concentrate primarily on results from the BRAHMS detector, one of the four major detectors at RHIC, but naturally also refer to results obtained by the other 3 experiments at RHIC (STAR, PHENIX and PHOBOS) insofar as they complement or supplement information obtained from BRAHMS. The BRAHMS experiment is a two arm magnetic spectrometer with excellent momentum resolution and particle identification capabilities for hadrons. The two spectrometers subtend only a small solid angle (a few msr) each, but they can rotate in the horizontal plane about the collision point enabling the collection of data on hadron production over a wide rapidity range (0-4), a unique feature among the RHIC experiments. For details about the BRAHMS detector system we refer the reader to [1,2].

2. What is a QGP and what does it take to see it?

The predicted transition from ordinary matter, which consists of hadrons inside which quarks and gluons are confined, to the QGP, a matter state in which quark and gluons are no longer confined to volumes of hadronic dimensions, can in the most simple minded approach be likened to the transition between two thermodynamic states in a closed volume.

As energy is transferred to the lower energy state a phase transition to the higher energy state occurs, akin to a melting or evaporation process. For a first order phase transition (PT), the transformation of one state into the other occurs at a specific temperature, termed the critical temperature, and the process is characterized by absorption of latent heat during the phase conversion leading to a constancy or discontinuity of certain thermodynamic variables as f.ex. the energy density is increased. In this picture it is tacitly assumed that the phase transition occurs between states in thermodynamic equilibrium. From such thermodynamic considerations and from more elaborate models based on the fundamental theory for the strong interaction, Quantum Chromo Dynamics (e.g. lattice QCD calculations), estimates for the critical temperature and the order of the transition can made. Calculations indicate that the critical temperature should be $T_c = 150 - 200MeV$ in the case of vanishing baryon chemical potential. In general, a decreasing critical temperature with increasing chemical potential is expected. Likewise, at non-zero chemical potential a mixed phase of coexisting HG and QGP is predicted to exist in a certain temperature interval around the critical temperature. Recently calculational techniques have progressed to allow an extension of the lattice methods also to finite chemical potential.

The transition between ordinary matter (the hadron gas, HG) to the QGP is thus primarily a deconfinement transition. However, it is also expected, due to the vanishing interaction between partons in the QGP phase, that hadrons masses will be strongly modified and in fact lowered. In the limit the hadrons are massless and thus identical (chiral symmetry). As a consequence of the QGP to HG transition the chiral symmetry is broken and the hadrons acquire a definite mass. Thus the transition is also a chiral symmetry transition. General theoretical arguments have been advanced for the equivalence of the critical temperature for chiral symmetry restoration and deconfinement (ref.–check).

It is, however, not at all clear that the transition to QGP as it is expected to be recreated in nucleus-nucleus collisions proceeds between states of thermodynamic equilibrium as sketched above. The reaction, from first contact of the colliding nuclei to freeze-out of the created fireball, occurs on a typical timescale of less than 10 fm/c and is governed by complex reaction dynamics so that non-equilibrium features are important. Likewise there is significant reinteraction of the strongly interacting components of the system, after its formation, that tend to smoothen specific features associated with a phase transition.

Many potential experimental signatures for the existence of the QGP have been proposed. These can be roughly grouped into two classes: 1) *evidence for bulk properties consistent with QGP formation*, e.g. large energy density, entropy growth, plateau behavior of the thermodynamic variables, unusual expansion and lifetime properties of the system, presence of thermodynamic equilibration, fluctuations of particle number charge etc, and 2) *evidence for modifications of specific properties of particles though to arise*

from their interaction with a QGP, such as the modification of widths and masses of resonances, modification of particle production probabilities due to color screening (e.g. J/Psi suppression) and modification of parton properties due to interaction with other partons in a dense medium (e.g. jet quenching), etc.

We may now ask the following questions: 1) what is the requirement for calling a state of matter a QGP?, and 2) what would constitute proof of QGP formation according to that definition?

As far as the first question is concerned it would seem obvious that the the determining factor is whether the high density state that is created in the nuclear collisions clearly has properties that are determined by its partonic composition, beyond what is known at the nucleon level in elementary nucleon-nucleon collisions (e.g. p+p collisions). It has often been presupposed that the 'plasma' should be in thermodynamical equilibrium. However, it does not appear to be essential that equilibrium should be established as long as the system under consideration is one of partons without imposed hadronic boundaries. Finally, it may be asked whether chiral symmetry restoration is essential. It would seem that even in a situation in which the partons of the system are still (strongly) interacting one may speak of QGP as long as the constituents are not doomed to a specific address inside individual hadrons. Thus it would seem that *deconfinement* is the foremost property needed to define the QGP state, and the one that needs to be proven by experiment.

Clearly, the observation of all, or at least of a number of the effects listed above, in a mutually consistent fashion, would seem to constitute a strong evidence for the formation of a QGP, as long as the observed effects can be unambiguously related to expected properties of the QGP state. In particular, the observed effects must not be also describable within other frameworks, f.ex. based on purely hadronic interactions, e.g. not explicitly involving the partonic degrees of freedom. This suggests the requirement that a 'proof', in addition to consistency with QGP formation, also must contain elements that are *only* describable in terms of QGP formation, phase transition etc.

Finally, if a sufficiently good case exists, we may also ask if there are any specific features that may *falsify* the conclusion. To our knowledge no tests have been proposed that may allow to falsify either a partonic scenario or a hadronic scenario, but it would be important if any such exclusive tests were to be formulated.

3. Reactions at RHIC: how much energy is released?

The stopping of atoms in matter is a long standing subject. A more recent one is the stopping of nuclei in collisions with each other. For the subject at hand the degree of stopping, i.e. loss of kinetic energy, between two colliding nuclei determines the amount of energy that can be converted into a material state such a the QGP.

A useful way to quantify the stopping is by the rapidity loss experienced by the baryons in the colliding nuclei. Rapidity is defined as

$$y = \frac{1}{2} ln(\frac{E + p_z}{E - p_z}) = \frac{1}{2} ln(\frac{1 + \beta cos\theta}{1 - \beta cos\theta}) \quad (1)$$

where E, pz, β and θ denote the total energy, longitudinal momentum, velocity and angle relative to the beam axis, respectively, of a particle. If incoming beam baryons have

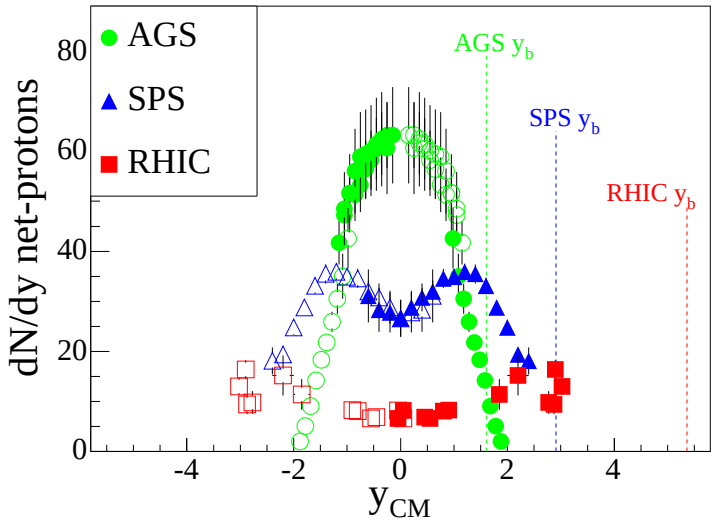

Figure 1. Preliminary rapidity densities of net protons (i.e. number of protons minus antiprotons) measured at AGS, SPS, and RHIC(BRAHMS). At RHIC, the full distribution cannot be measured with current experiments, but BRAHMS will be able to extend its measurements to y=3.5 in coming runs, corresponding to measurements at 2.3 degrees with respect to the beam.

rapidity, y_b relative to the CM (which has $y = 0$) and average rapidity

$$< y >= \int_0^{y_b} y \frac{dN}{dy} dy \tag{2}$$

after the collision, the rapidity loss is $\delta y = y_b - < y >$. Here dN/dy denotes the number of particles per unit of rapidity. Thus, for the extreme case of full stopping: $\delta y = y_b$. This corresponds to the situation found at very low energies where all the beam baryons loose all their kinetic energy. In the expression above a complication arises at CM energies large enough to allow for the formation of baryon-antibaryon pairs. Thus the baryon dN/dy distribution to be used is that for the net number of baryons (i.e. the difference between the number of baryons and antibaryons).

At AGS energies the number of produced antibaryons is quite small and the the net-baryon distribution is similar to the proton distribution. The net-proton rapidity distribution is centered around $y = 0$ and is rather narrow. The rapidity loss is about 1 for a beam rapidity of approx. 1.6. At CERN-SPS energies ($\sqrt{s_{NN}}$ = 17 GeV, 158 AGeV Pb+ Pb reactions) the rapidity loss is about 2 for a beam rapidity of 2.9, about the same relative rapidity loss as at AGS. The fact that the rapidity loss is large on an absolute scale means, however, that there is still a sizeable energy loss of the colliding nuclei. This energy is available for particle production and other excitations. Indeed, in collisions at SPS, multiplicities of charged hadrons are about dN/dy=180 around y=0. At SPS another feature is visible (see fig. 1): the net proton rapidity distribution shows a double 'hump' with a dip around y=0. This is a consequence of two effects: the finite rapidity loss of the colliding nuclei and the finite width of each of the humps, which reflect the rapidity distributions of the protons in the colliding nuclei after the collisions. This pic-

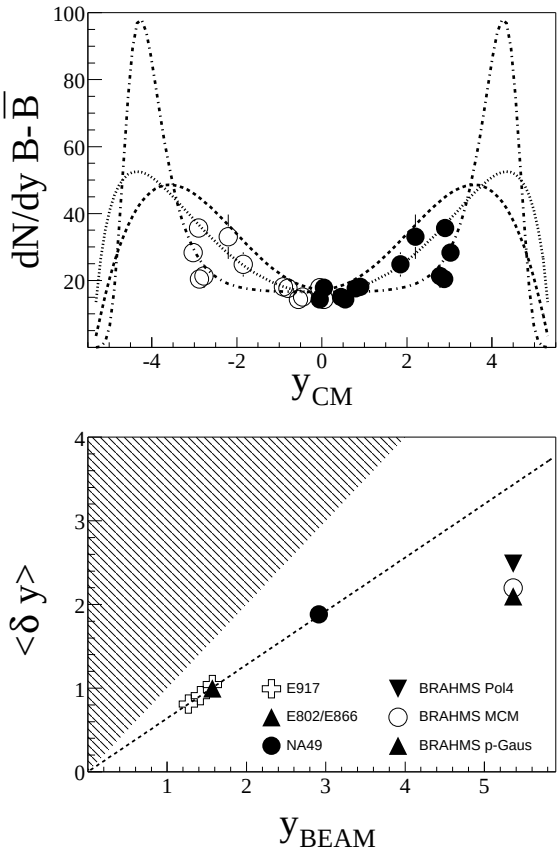

Figure 2. Upper panel: estimates of possible net-baryon distributions requiring baryon number conservation. We have assumed that $N(n) \approx N(p)$ and scaled hyperon yields at midrapidity to forward rapidity using HIJING. From these extremes, limits on the rapidity loss of colliding Au ions at RHIC can be set (lower panel). The BRAHMS data are preliminary.

ture suggests that the reaction at SPS is beginning to be transparent in the sense that fewer of the original baryons are found at midrapidity after the collisions, in contrast to the situation at lower energies.

BRAHMS has measured the net proton rapidity distribution at RHIC in the interval $y = 0 - 3$ in the first run with (0-10%) central Au+Au collisions at full energy. The beam rapidity at RHIC is about 5.4. Details of the analysis may be found in refs.[3]. The results are displayed in fig. 9 together with the previously discussed net-proton distributions measured at AGS and SPS. It is notable that the RHIC distribution is both qualitatively and quantitatively different from those at lower energies.

The net number of protons per unit of rapidity around y=0 is only about 7 and the distribution is flat over at least the first unit of rapidity. The distribution increases in the rapidity range $y = 2 - 3$ to an average $dN/dy \approx 12$. We have not yet completed the measurements at the most forward angles (highest rapidity) allowed by the geometrical setup of the experiment, but we can exploit that there must be baryon conservation in the reactions to try to set limits on the relative rapidity loss at RHIC. This is illustrated

in fig. 2, which shows various possible distributions whose integral areas correspond to the number of baryons present in the overlap between the colliding nuclei. From such distributions one may deduce a set of upper and lower limits for the rapidity loss at RHIC. In practice the situation is complicated by the fact that not all baryons are measured. We measure in BRAHMS the direct protons, but only some of the decay protons from for example Λ. The limits shown in the figure include some reasonable estimates of these effects [3,6]. The conclusion is that the *absolute* rapidity loss at RHIC ($\delta y = 2.2 \pm 0.4$) is not appreciably larger than at SPS. In fact the *relative* rapidity loss is significantly reduced as compared to an extrapolation of the low energy systematics [4].

It should be noted that the rapidity loss is still significant and that, since the overall beam energy (rapidity) is larger at RHIC than at SPS, the *absolute energy loss* increases appreciably from SPS to RHIC thus making available a significantly increased amount of energy for particle creation in RHIC reactions.

In particular we have found that the average energy loss of the colliding nuclei corresponds to about 73 ± 6 GeV per nucleon. From our measurements of the particle production as a function of rapidity (pions, kaons and protons and their antiparticles) we can deduce not only the number of produced particles but also their average transverse momentum and thus their energy. Within systematic errors of both measurement we find that the particle production is consistent with the energy that is taken from the beam.

Thus the energy loss measurements clearly establish that as much as 26 TeV kinetic energy is removed from the beam pr. central Au+Au collision. This energy is available for particle production in a small volume immediately after the collision.

4. Particle production and energy density

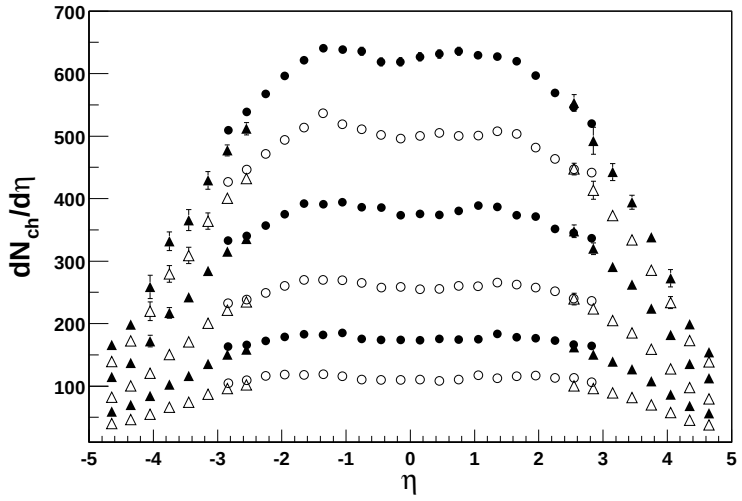

Figure 3. Pseudorapidity densities (multiplicities) of charged particles measured by BRAHMS for $\sqrt{s_{NN}}$ = 200 GeV) Au+Au collsions. The various distributions correspond to collisions centralities 0-5% (top), 5-10%,10-20%,20-30%,30-40%, 40-50%. The integral of the most central distribution corresponds to about 4600 charged particles [2].

Figure 4. Multiplicity of charged particles per participant pair as a function of number of participants (collisions centrality). Lines show...

The stopping scenario that we observe at RHIC and which was outlined in the previous section entails that the reaction can be viewed as quite transparent (opaque is perhaps a better word). After the collision, the matter and energy distribution can be conceptually divided up into two main parts, namely a so-called fragmentation region consisting of the excited remnants of the colliding nuclei which have experienced an average rapidity loss of about 2.2 and a central region in which few of the original baryons are present but where significant energy density is collected. This picture is consistent with the schematic one already proposed by Bjorken 20 years ago [5].

The central region (an interval around midrapidity) is decoupled from the fragments. The energy removed from the kinetic energy of the fragments is initially stored in a color field strung between the receeding partons that have interacted. The linear increase of the color potential with distance eventually leads to the production of quark-antiquark pairs. Such pairs may be produced anywhere between the interacting partons leading to an approximately uniform particle production as a function of rapidity. In this picture, the properties of the particle production is also uniform as a function of rapidity (boost invariance). If the density of produced quark-antiquark pairs is sufficiently high, the average distance between them will be low and the binding potential between the colored objects will be small. The objects will become asymptotically free and exist in a plasma like state until the subsequent expansion and lowered density leads to confinement and hadronization.

Figure 3 shows the overall multiplicity of charged particles observed in Au+Au collisions at RHIC [2,7] for various collision centralities and as a function of pseudorapidity (pseudorapidity, η, is defined as $\eta = ln(cot(\theta/2))$ and is a customary rapidity variable for non identified particles). The figure shows that the multiplicity at RHIC is about $dN/d\eta = 625$ charged particles pr. unit rapidity around $\eta = 0$ for central collisions. The production of charged particles in central collisions exceeds the particle production seen in p+p collisions at the same energy by about 40%, when the yield seen in p+p collisions is multiplied by the number of participant nucleon pairs in the overlap region between the colliding nuclei.

Figure 5 shows a recent and more detailed study of the particle production in central

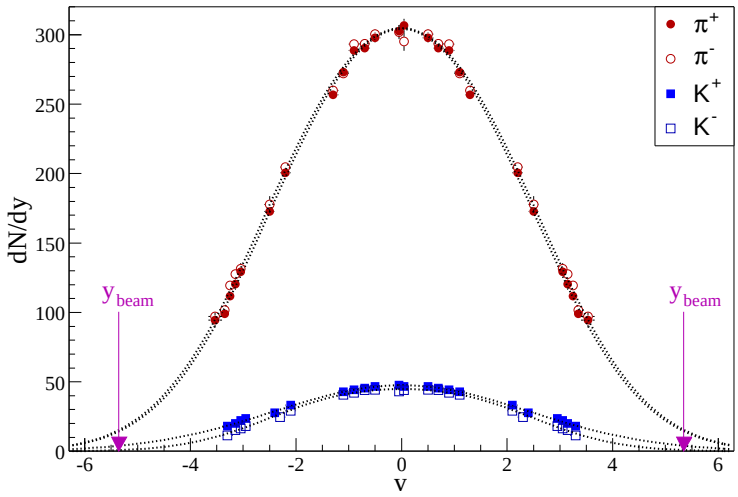

Figure 5. Rapidity density distribution for positive and negative pions and kaons. Data points collected at positive y have been reflected around y=0. GET NEWER PLOT FROM DJAMELS PAPER

collisions as a function of rapidity [14]. The figure shows the rapidity densities of pions and kaons for central collisions. From such distributions we can construct the ratio of the yields of particles and their antiparticles as a function of rapidity. Figure 6 shows the ratios of yields of antihadrons to hadrons (posititive pions, kaons and protons and their antiparticles). The ratio is seen to be approaching unity in an interval of about 1.5 units of rapidity around midrapidity, suggesting that the particle production is predominantly from pair creation. This is exactly true for pions (ratio of 1), but less so for kaons (ratio= 0.95) and protons (ratio= 0.76). The reason is that there are other processes that break the symmetry between particles and antiparticles that depend on the net-baryon distribution discussed in the previous section. One such process that is relevant for kaons is the associated production mechanism (e.g. $p + p \rightarrow p + \Lambda + K^+$) which leads to an enrichment of positive kaons in regions where there is an excess of baryons. Support for this view is given by fig. 7, which shows the systematics of kaon production relative to pion production as a function of center of mass energy. At AGS, where the net proton density is high at midrapidity, the rapidity density of K^+ strongly exceeds that of K^-. In contrast, at RHIC, production of K^+ and K^- is almost equal. This situation changes, however, at larger rapidities where the net proton density increases.

Integration of the charged particle pseudorapidity distributions corresponding to central collisions tells us that about 4600 charged particles are produced in each of the 5% most central collisions. Since we only measure charged particles, which are predominantly pions and kaons, as may be seen from fig. 5, and not the neutrals, we multiply this multiplicity by 3/2 to obtain the total particle multiplicity of about 7000 particles.

From the measured spectra of pions, kaons and protons and their antiparticles as a function of transverse momentum we can determine the average transverse momentum for each particle species (fig. 8). This allows us to estimate the initial energy density from

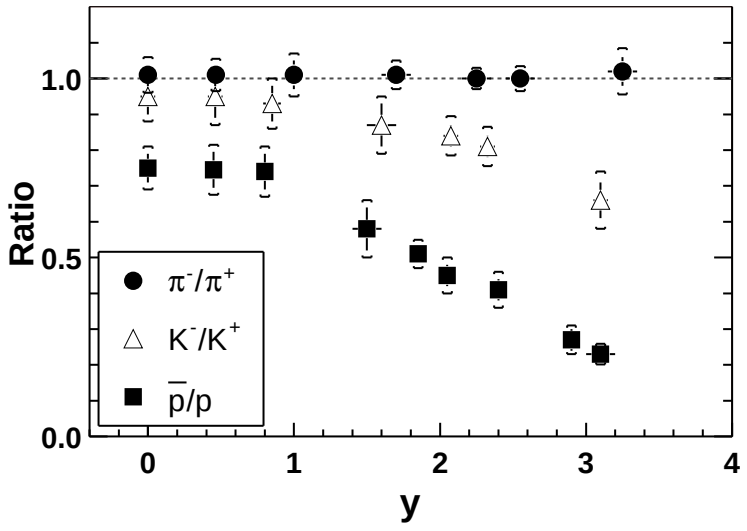

Figure 6. Ratios of antiparticles to particles (pions, kaons and protons) as a function of rapidity for $\sqrt{s_{NN}}$ = 200 GeV Au+Au collisions measured by the BRAHMS experiment [8]. For the first time in nuclear collisions an approximate balance between particles and antiparticles is seen around midapidity.

Bjorkens formula:

$$\epsilon = \frac{1}{\pi R^2 \tau} \frac{d < E_t >}{d\eta} \tag{3}$$

where we can make the substitution $d < E_t >=< m_t > dN$ and use quantities from the measured spectral distributions. Since we wish to calculate the energy density in the very early stages of the collision process we may use for R the radius of the overlap disk between the colliding nuclei, thus neglecting transverse expansion. The formation time is more tricky. It is often assumed to be of the order of 1 fm/c, a value that may be inferred from the uncertainty relation an the typical relevant energy scale (200 MeV). Under these assumptions we find that $\epsilon > 5 GeV/fm^3$. This value of the initial energy exceeds by a factor of 30 the energy density of a nucleus, by a factor of 10 the energy density of a baryon and by a factor of 5 the critical energy density for QGP formation that is predicted by lattice QCD calculations.

We may argue that the time at which the energy density should be estimated is the time relevant for the passage of the two nuclei through each other. As seen from the CM frame (which, for Au+Au collisions, is identical with the laboratory frame of reference) the nuclei are Lorentz contracted by a factor of 100, thus only having longitudinal thicknesses of the order of 0.15 fm. The typical traversal time is thus of the order of 0.15 fm/c. This leads, utilizing the equation above, to an estimated initial energy density of about $35 GeV/fm^3$. This value exceeds by a factor of about 70 the energy density of the baryon and by a factor of 35 the expected critical density.

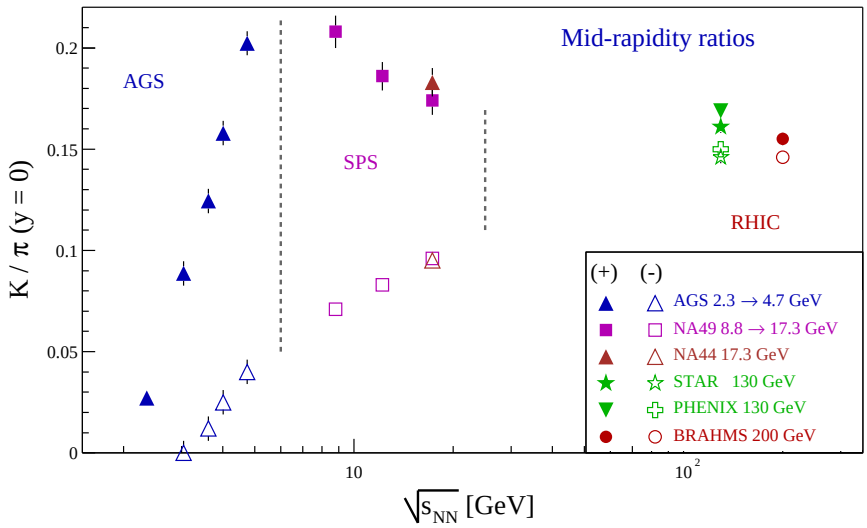

Figure 7. Ratios of kaons and pions of both charge signs as a function of center of mass energy in the nucleon-nucleon system at midrapidity. At top RHIC energy the two ratios are about the same and equal to 0.15. Preliminary BRAHMS data.

5. The size of the fireball at RHIC.

The space time extend of the particle emitting source at RHIC can be probed through studies of two particle correlations, f.eks . HBT interferometry or multibaryon coalescence. BRAHMS has studied the latter (ref. Marco thesis) via the ratio of the production yields of deuterons to protons and antideuterons to antiprotons. The resulting coalescence factors can be related to a volume of homogeneity or correlation lengths between the involved particles. This volume is in the case of the deuterons characteristic of the conditions at freeze out, as the small deuteron binding energy (2.2 MeV) only allows binding in the very last stages of the system expansion. HBT analyses yield similar spatial information. A characteristic feature of such measurements at RHIC is that the extracted volumes or radii are no significantly different at RHIC than at SPS.

HBT also provides information on the lifetime of the particle emission by comparing radii along and perpendicularly to the expansion direction (R_{out} and R_{side}). The results indicate that the system lifetime is short (comparable to that found by similar analyses at SPS energies) and thus at variance with early expectations for a long lived QGP state.

6. Is there thermodynamical and chemical equilibrium at RHIC?

It has traditionally been seen considered important to determine whether there is thermodynamical equilibration of the 'fireball', in relativistic collisions in general, and at in RHIC in particular. The main reason is that, if there is thermalization, the simple two phase model may be invoked and the system should evidence the recognizable features of a phase transition. In nuclear collisions, however, the time scale available for equilibration is very short and the entire system only lives in the order of 10 fm/c. Consequently, it is not evident that the system evolves through equilibrated states. Conversely, if equilibrium is established, it would suggest that the system existed for a short time in a state with

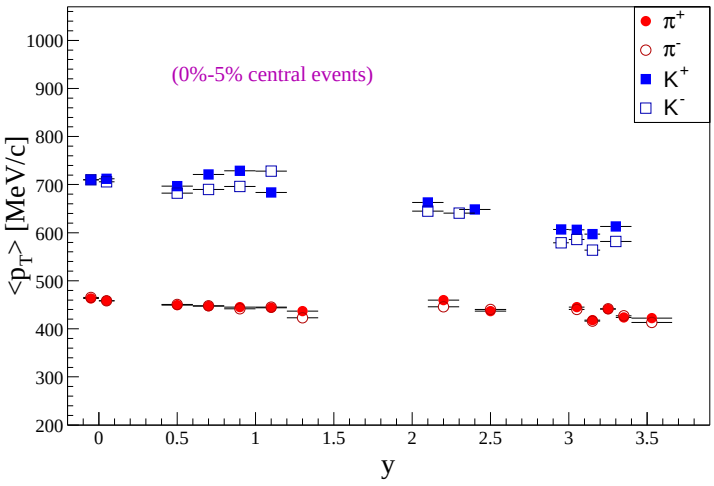

Figure 8. Distribution of average transverse momenta of pions and kaons as a function of rapidity as measured by BRAHMS. Preliminary.

Figure 9. B2 for D and anti D at RHIC. Preliminary. FROM MARCOS THESIS.

sufficiently short mean free path. A central issue is whether equilibrium is established in the hadronic cloud in the later stages of the collsions just prior to freeze-out or whether it is established on a partonic scale prior to hadronization. Thus, even if equilibration *per se* is not a requirement for defining the QGP, it may prove to be an important tool in *identifying* the QGP.

6.1. Particle yields

The particle yields measured by BRAHMS also lend themselves to an analysis of the charged particle production in terms of the statistical model [8],[9–12]. Figure 10 shows the ratios of negative kaons to positive kaons as a function of the corresponding ratios of antiprotons to protons for various rapidities at RHIC. The data are for central collisions, and the figure also displays similar ratios for heavy ion collisions at AGS and SPS energies.

There is a striking correlation between the RHIC/BRAHMS kaon and proton ratios over 3 units of rapidity. Assuming that we can use statistical arguments based on chemical and thermal equilibrium at the quark level, the ratios can be written

$$\frac{\rho(\bar{p})}{\rho(p)} = exp(\frac{-6\mu_{u,d}}{T}) \tag{4}$$

and

$$\frac{\rho(K^-)}{\rho(K^+)} = exp(\frac{-2(\mu_{u,d} - \mu_s)}{T}) = exp(\frac{2\mu_s}{T}) \times [\frac{\rho(\bar{p})}{\rho(p)}]^{\frac{1}{3}} \tag{5}$$

where ρ, μ and T denote number density, chemical potential and temperature, respectively. From equation 4 we find the chemical potential for u and d quarks (often called the baryochemical potential) to be around 25 MeV, the lowest value yet seen in nucleus-nucleus collisions. Equation 5 tells us that for a vanishing strange quark chemical potential we would expect a power law relation between the two ratios with exponent 1/3. The observed correlation is well described by the relationship $\rho(K^-)/\rho(K^+) = \rho(\bar{p})/\rho(p)^{0.24}$, i.e. with an exponent that is close to 1/4 suggesting, a finite value of the strange quark chemical potential.

A more elaborate analysis for a grand canonical ensemble assuming charge, baryon and strangeness conservation can be carried out by fitting these and many other particle ratios observed at RHIC by the 4 experiments in order to obtain the chemical potentials and temperatures. It is found that a very large collection of such particle ratios are extremely well described by the statistical approach.

An example of such a procedure is shown in fig. 10 and displayed with the full line [13]. Here the temperature is 170MeV. The point to be made here is that the calculation agrees with the data over a wide energy range (from SPS to RHIC) and over a wide range of rapidity at RHIC. This may be an indication that the system is in chemical equilibrium over the considered $\sqrt{s}$ and y ranges (or at least locally in the various y bins). Separate measurements at RHIC of, for example, elliptical flow also point to local equilibration around midrapidity.

6.2. Flow

The properties of the expanding matter in the later stages of the collisions up to the moment when reinteractions cease (kinetic freeze out) can be studied from the momentum distribution of the emitted particles.

Analysis of the slopes of spectra of emitted particles depend in general on the temperature of the source from which they were created and on kinetic effects that may alter the expected Maxwellian distribution, such as a velocity component resulting from an outwards pressure leading to an outwards flow of the matter. This flow is expected, in the case of (at least local) thermal equilibrium and sufficient density, to be describable by concepts derived from fluid dynamics. It is to be noted that the slopes of spectra reflect the particle distributions at the time when reinteractions have ceased and thus the obtained physical quantities should be associated with conditions at freeze-out.

The simplest analysis parametrizes the inverse slopes of particle spectra (the apparent temperature) as the sum of a thermal term and a kinetic (flow) term ($T_{eff} = T_{th} + m <$

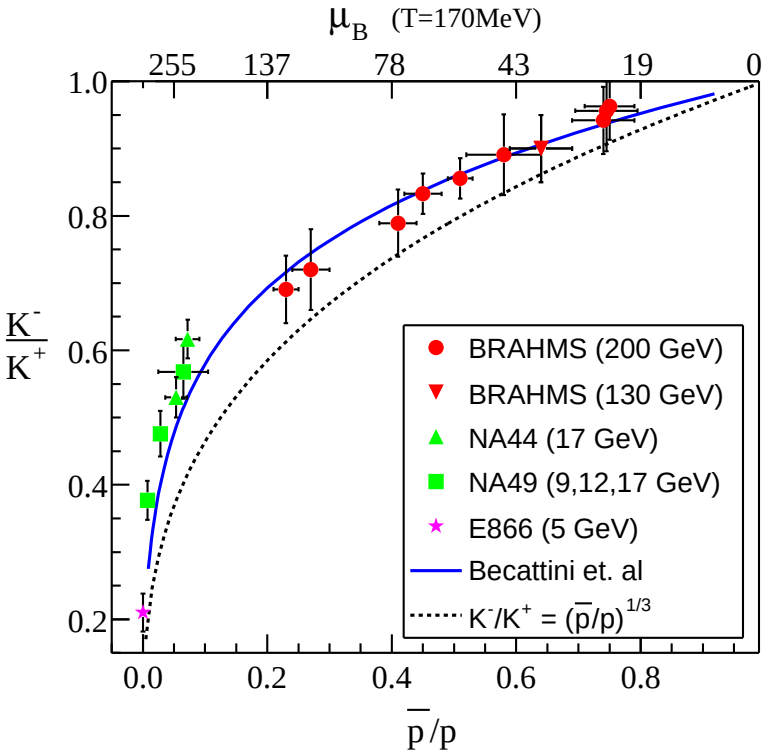

Figure 10. Correlation between the ratio of charged kaons and the ratio of antiprotons to protons. The dashed curve corresponds to equation 3 in the text. The full drawn curve is a statistical model calculation with a chemical freeze-out temperature of 177MeV.

$\beta >^2$, where m and $< \beta >$ are the particle rest mass and its average transverse flow velocity. A more refined analysis employs a parametrization of the spectrum shape which also includes a description of the radial dependence of the flow velocity (the so-called blastwave approach). The result of such analyses performed simultaneously on several particle/antiparticle species indicates that the thermal (freezeout) temperature is in the range T= 120-140 MeV and that the average flow velocity is about $0.5c - 0.6c$. The first quantity is found, as expected, to be lower than the temperature of the chemical freeze out discussed in the previous subsection. Indeed, it would be expected that the freeze-out of particle ratios occurs earlier than the kinetic freeze out of the particles. The flow velocity component is substantially larger than what was observed, f.ex at SPS energies. This is consistent with a large pressure gradient in the transverse direction resulting from a large initial density.

Fig.11 shows results from analysis of particle spectra around midrapidity by the BRAHMS experiment using the blastwave approach.

Another useful tool to study the thermodynamic properties of the source is the analysis of the azimuthal momentum distribution of the emitted particles relative to the event plane (defined as the direction of the impact parameter). This distribution is usually parametrized as a series of terms depending on $cos(n(\phi - \phi_r))$. The coefficient (v_1) to the n=1 term measures the so-called directed flow and the coefficient (v_2) to the n=2 term measures the elliptic flow. Elliptic flow has been analyzed at RHIC (refs...) and has been found to reach large (v_2) values consistent with the hydrodynamical limit and

Figure 11. Analysis of particle slopes at midrapidity... Preliminary.

thus of equilibration. It has been proposed (refs.) that in view of the short lifetimes of the system deduced from particle correlation studies (HBT, coalescence etc.) that the equilibration that is deduced from the mentioned analyses can only be established at the *partonic* level when the system is very dense and has many more particles (degrees of freedom). This explanation presupposes however that there are many reinteractions and thus that the dense partonic phase is still strongly interacting.

7. High pt suppression. The smoking gun of QGP?

The discussion in the previous sections indicates that the conditions for particle production in a interval $|y| < 1.5 - 2$ at RHIC are radically different than for reactions at lower energies. At RHIC the central zone is nearly baryon free, the considered rapidity interval appears to approximately exhibit the anticipated boost invariant properties, the particle production is large and dominated by pair production and the energy density appears to exceed significantly the one required for QGP formation. The overall scenario is therefore consistent with particle production from the color field, formation of a QGP and subsequent hadronization. Correlation studies suggest that the lifetime of the system is short ($< 10 fm/c$) and, for the first time, there is strong evidence suggesting thermodynamical equilibrium already at the partonic level.

But, is this interpretation unique? And, can more mundane explanations based on a purely hadronic scenario be excluded? In spite of the obvious difficulties in reconciling the high initial energy density with hadronic volumes, a comprehensive answer to this question requires the observation of an effect that is directly dependent on the partonic or hadronic nature of the formed high density zone.

Such an effect has recently been discovered at RHIC and is related to the suppression of the high transverse momentum component of hadron spectra in central Au+Au collisions as compared to scaled momentum spectra from p+p collisions [16–19]. The effect, originally proposed by Bjorken, Gyulassy and others [5,26,25] is based on the expectation of a large energy loss of high momentum partons scattered in the initial stages of the col-

lisions in a medium with a high density of free color charges. According to QCD colored objects may loose energy by radiating gluons by bremsstrahlung. Due to the color charge of the gluons, the energy loss is proportional to the square of the length of color medium traversed. Such a mechanism would strongly degrade the energy of leading partons resulting in a reduced transverse momentum of leading particles in the jets that emerge after fragmentation into hadrons. The STAR experiment has shown that the topology of high pt hadron emission is consistent with jet emission, so that we may really speak about jet-suppression.

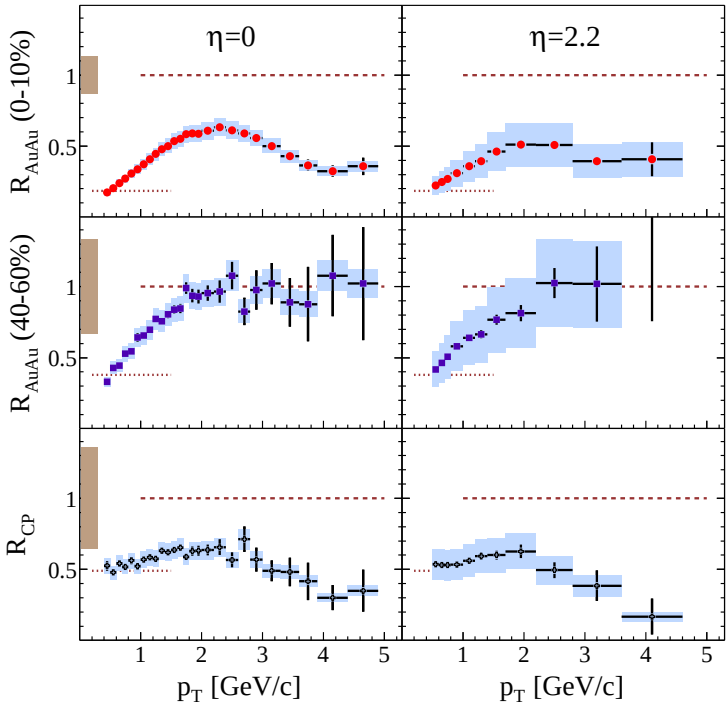

Figure 12. Nuclear modification factors R_{AuAu} as defined in the text, for central and semi-peripheral Au+Au collisions at midrapidity (left) and forward rapidity (right). The lower row shows the factor R_{cp}, i.e the ratio of the R_{AuAu} for central and peripheral collisions, which has the property of being independent of the p+p reference spectrum.

The two upper rows of fig. 12 show our [15,16] measurements of the so-called nuclear modification factors for *unidentified* charged hadrons from Au+Au collisions at rapidities $\eta = 0$ and 2.2. The nuclear modification factor is defined as:

$$R_{AA} = \frac{d^2N^{AA}/dp_t d\eta}{N_{bin} d^2N^{NN}/dp_t d\eta} \tag{6}$$

It involves a scaling of measured nucleon-nucleon transverse momentum distributions by the number of expected incoherent binary collisions, N_{bin} (see [20,21]. In the absence of any modification resulting from the 'embedding' of elementary collisions in a nuclear

collision we expect $R_{AA} = 1$ a high p_t. At low p_t, where the particle production follows a scaling with the number of participants, the above definition of R_{AA} leads to $R_{AA} < 1$ for $p_t < 2GeV/c$. In fact, it is found that $R_{AA} > 1$ for $p_t > 2GeV/c$ in nuclear reactions at lower energy. This effect, called the Cronin effect, is associated with initial multiple scattering of high momentum partons.

Figure 12 demonstrates that, surprisingly, $R_{AA} < 1$ also at high p_t for central collisions at both pseudorapidities, while $R_{AA} \approx 1$ for more peripheral collisions. It is remarkable that the suppression that is observed at $p_t \approx 4GeV/c$ is very large, amounting to a factor of 3 for central Au+Au collisions as compared to $p + p$ and a factor of more than 4 as compared to the more peripheral collisions. Such large suppression factors are observed at both pseudorapidities.

It has been conjectured that the observed high p_t suppression might be the result of an entrance channel effect, for example due to a limitation of the phase space available for parton collisions related to saturation effects [27] in the gluon distributions inside the swiftly moving colliding nucleons (which have $\gamma = 100$). As a test of these ideas we have determined the nuclear modification factor for 100 AGeV d + 100 AGeV Au minimum bias collisions. The resulting R_{dAu} is shown in fig. 13 where it is also compared to the R_{AuAu} for central collisions previously shown in fig. 12. No high-p_t jet suppression is observed for d+Au. In fact, the R_{dAu} distribution measured for d+Au shows the Cronin type enhancement [28] observed at lower energies [22–24]. At $p_t \approx 4GeV/c$ we find a ratio $R_{dAu}/R_{AuAu} \approx 5$. These observations are consistent with the smaller transverse dimensions of the overlap disk between the d and the Au nuclei and also appear to rule out initial state effects.

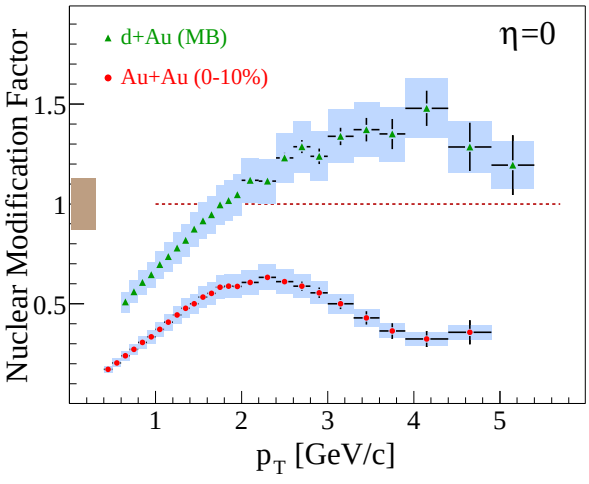

Figure 13. Nuclear modification factors measured for central Au+Au collisions and minimum bias d+Au collisions at $\sqrt{s_{NN}} = 200$ GeV, evidencing the important high pt suppression observed in central Au+Au collisions.

The very large suppression observed in central Au+Au collisions must be quantitatively understood and will require systematic dynamic modelling. At $\eta = 0$ the particles are emitted at 90 degrees relative to the beam direction, while at $\eta = 2.2$ the angle is only

about 12 degrees. In a naive geometrical picture of an absorbing medium with cylindrical symmetry around the beam direction, the large suppression seen at forward angles suggests that the suppressing medium is extended also in the longitudinal direction. Since the observed high p_t suppression is similar or even larger at forward rapidity as compared to midrapidity (see fig. 16) one might be tempted to infer a longitudinal extend of the dense medium which is approximately similar to its transverse dimensions ($R \approx 5fm$), and from this a life time longer than $5fm/c$. However, the problem is more complicated, due to the significant transverse and in particular longitudinal expansion that occurs as the leading parton propagates through the medium, effectively reducing the densities of color charges seen. Also high-pt suppression at forward rapidities may be expected due to the possible existence of a Color Glass Condensate phase in the colliding nuclei (see the discussion in the next section).

There is little doubt that systematic studies of the high p_t-jet energy loss as a function of the thickness of the absorbing medium obtained by varying the angle of observation of high p_t jets relative to the beam direction will be required in order to understand the properties of the dense medium. The BRAHMS experiment is uniquely suited among the RHIC experiments to carry out such a *QGP tomography*.

Figure 14. Plot of identified high pt from QM04. Preliminary.

Due to its excellent particle identification capabilities BRAHMS can also study the dependence of the high-pt suppression on the type of particle. Preliminary results (ref. qm2002, qm2004) indicate that mesons (pions and kaons) experience high pt suppression while baryons (protons) do not. The reason for this difference is a present not understood. It may be due to details in the fragmentation mechanism that leads to different degrees of suppression for 2 quark and 3 valence quark systems. It may also be due to the fact that baryons, due to their larger mass, are more sensitive to flow than mesons. Consequently, the pt- spectrum for these particles is flatter than for mesons, thus compensating for a possible high pt suppression similar to that seen for the mesons. These questions can and will be addressed in detail through the analysis of the large data set collected by

BRAHMS in the high luminosity Au+Au run of year 2004.

Figure 15. Plot of 63 GeV high pt supp. Preliminary.

Finally, we mention that the short commissioning run for Au+Au collisions at $\sqrt{s_{NN}} = 62.4$ GeV has allowed us to carry out a first and preliminary analysis of the high pt suppression of charged hadrons at an energy of about 1/3 maximum RHIC energy and about 3.5 times the maximum SPS energy. Preliminary results are shown in figure **??** for nuclear modification factor calculated for the sum of all charged hadrons measured at 45 degrees($\eta = 1.1$) with respect to the beam direction. The data have been compared to reference spectra measured in $\sqrt{s_{NN}} = 63$ GeV p+p collisions at the CERN-ISR. Figure **??** shows that the degree of high pt suppression at the lower energy is less important than at $\sqrt{s_{NN}} = 63$ GeV. For comparison, at SPS energies no high pt suppression was observed.

8. The color glass condensate: a model for the initial state of nuclei?

As part as the study of the high pt suppression in nucleus-nucleus collisions BRAHMS has investigated the rapidity dependence of the nuclear modification factors as a function of rapidity ($\eta = 0, 1, 2.2, 3.2$) in d+Au collisions at $\sqrt{s_{NN}} = 200$ GeV. As discussed in the previous section the modification factors are consistent with the absence of high pt suppression around midrapidity. This may be taken as evidence for the fact that the high pt suppression seen in Au+Au collisions is not due to particular conditions in the colliding nuclei (initial state effects).

At forward rapidity, however, BRAHMS has measured, in d+Au collisions, a marked high-pt suppression starting already at $\eta = 1$ and increasing smoothly in importance with increasing pseudorapidity (up to $\eta = 3.2$). It has been proposed that this effect at forward rapidity is related to the initial conditions of the colliding d and Au nuclei in particular to the existence of the Color Glass Condensate (CGC).

The CGC is a proposed description of the ground state of the nuclei prior to collisions.

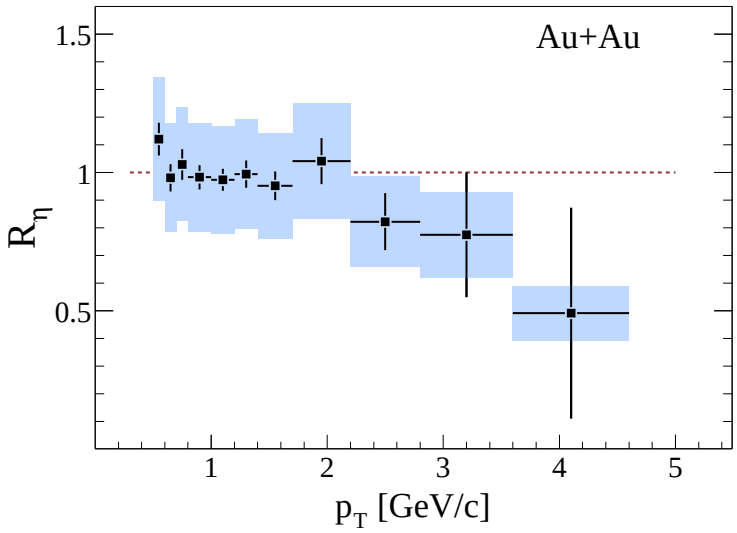

Figure 16. Ratio, R_η, of the suppression factors R_{cp} at pseudorapidities $\eta = 0$ and $\eta = 2.2$ shown in figure 9. The figure suggest that high p_t suppression persists (and is even more important) at forward rapidity than at $\eta = 0$.

The basic idea is, that nuclei contain a large number of low-x gluons (x is the fraction of the nucleon momentum carried by the considered parton) that appears to diverge with decreasing x. At small x however the gluon wavefunctions in the colliding nuclei are highly delocalized, thereby enabling gluon-gluon interactions (gluon fusion) leading to a depletion of the number of low x gluons in a certain p-t range. This mechanism prevents an 'infrared catastrophe', since the number of low-x gluons saturates. Such effects are seen in lepton-hadron collisions at HERA (refs. xxx).

Figure 17. Nuclear modification factors measured in d+Au collisions at pseudorapidities $\eta = 0, 1, 2.2, 3.2$ for central collisions.

In the McLerran-Venugopalan approach [**?**] the transverse momentum transfer scale for the onset of gluon saturation depends on the gluon density (and thus on the number of participating nucleons), and is connected with the rapidity (y) of measured particles by $Q_s^2 \sim A^{\frac{1}{3}} e^{\lambda y}$ suggesting that saturation effects may best be studied at large y, or at large values of the related pseudorapidity $\eta = -ln(tan(\frac{\theta}{2}))$, i.e at small angles θ relative to the beam direction.

Collisions between heavy ions with energies E=100$AGeV$ at the Relativistic Heavy Ion Collider (RHIC) as observed by provide a window to the low-x gluon distributions of swiftly moving nuclei. In particular, head-on collisions between deuterons and gold nuclei in which hadrons, produced mostly in gluon-gluon collisions, are detected, as in BRAHMS, close to the beam direction but away from the direction of motion of the gold nuclei, allow to probe the low-x components of the wave function of the gold nuclei.

Figure xxx shows the nuclear modification factors obtained at the 4 rapidities for d+Au collisions. At present quantitative theoretical predictions of this effect are not available, but the observations seem to be supported in a qualitative fashion by the CGC model. However a more detailed understanding of this phenomenon requires comparison to quantitative predictions of the various models on the market (e.g. CGC, gluon shadowing, hadronic models).

Figure 18. Plot of RCp in d+Au.

Most recently we have carried out the first analysis of the nuclear modification factors for $\sqrt{s_{NN}} = 200$ GeV Au+Au collisions in the rapidy range $\eta = 2.9 - 3.5$ from the 2004 RHIC run. The results are consistent with the persistence of high pt suppression into this rapidity range for Au +Au collisions, thus suggesting that there may be two competing mechanisms responsible for the observed high p-t suppression in energetic Au+Au collisions, each active in its particular rapidity window.

9. Conclusions and perspectives

The results from the first round of RHIC experiments has clearly shown that we have moved in high energy nucleus-nucleus collisions into a qualitatively new physics domain characterized by a high degree of reaction transparency leading to the formation of a near baryon free central region . There is, in spite of this, appreciable energy loss of the colliding nuclei, so the conditions for the formation of a very high energy density zone with approximate balance between matter and antimatter, in an interval of $|dN/dy| < 2 \pm 0.5$ around midrapidity are present. The indications are that the initial energy density is considerably larger than $5GeV/fm^3$, i.e. well above the energy density at which it begins to be difficult to conceive of hadrons as isolated and well defined entities. This together with the evidence for short system lifetimes and equilibration is consistent, calling also on theoretical arguments, with the formation of a system containing a high number of quarks and gluons that have interacted and shared energy.

Consistency, however, is not the same as proof. In order to prove the creation of the deconfined state we must find isolate observables that can only acquire the observed values if deconfinement is present. A very strong candidate for this is the hight-pt jet suppression observed by the 4 RHIC experiments, whose remarkably large magnitude seems only to be explainable by a scenario in which partons loose energy as they traverse a medium with a high density of color charges. An important part of the proof therefore has to rely on the unambiguity of the results of theoretical modelling of the entire reaction. While the experimental results at the present state of affairs appear to be unambiguous, the same can probably not be said of the theroretical situation.

Much hope has been ... PT... bla-bla.... Here we must conclude on what OUR opinion is.

10. Acknowledgements

This work was supported by the Danish Natural Science Research Council, the division of Nuclear Physics of the Office of Science of the U.S. DOE, the Research Council of Norway, the Polish State Committee for Scientific Research and the Romanian Ministry of Research.

REFERENCES

1. M. Adamczyk *et al.*, BRAHMS Collaboration, Nucl. Instr. and Meth., **A499** (2003) 437.
2. I. G. Bearden *et al.*, BRAHMS Collaboration, Phys. Lett. **B523**, 227 (2001) and Phys. Rev. Lett. **88**, 202301 (2002).
3. BRAHMS collaboration Nucl. Phys. A**715**, 171c (2003) and *ibid* p. 482c, and P. Christiansen, Ph. D. thesis, Univ. Copenhagen, June 2003.
4. Phys. Rev. **C52**, 26(1995).
5. J. D. Bjorken, Phys. Rev. D**27**, 140 (1983).
6. C. Adler *et al.*, STAR Collaboration, Phys. Rev. Lett. **89**, 092301 (2002) and K. Adcox *et al.*, PHENIX collaboration, ibid p. 092302.
7. B. B. Back *et al.*, PHOBOS Collaboration, Phys. Rev. Lett. **88**, 022302 (2002).

8. I. G. Bearden *et al.*, BRAHMS Collaboration, Phys. Rev. Lett. **90**, 102301 (2003) and Phys. Rev. Lett. **90**, 112305 (2003) and refs. therein.
9. P. Koch *et al.*, Phys. Rep. **142** (1986) 167.
10. J. Cleymans *et al.* Z. Phys. **C57** (1993) 135.
11. J. Cleymans *et al.* Nucl. Phys. **A566** (1994) 391.
12. P. Braun-Munzinger *et al.*, Phys. Lett. B **518**, 41 (2001).
13. F. Becattini *et al.*, Phys. Rev. C**64**, 024901 (2001)and private communication.
14. D. Ouerdane, Ph.D. thesis, Univ. Copenhagen, August 2003.
15. BRAHMS collaboration Nucl. Phys. A715 741c (2003).
16. A. Arsene et al. Phys. Rev. Lett **91**, 072305 (2003).
17. C. Adler et al. Phys. Rev. Lett. **89**, 202301(2002) and Phys. Rev. Lett **91**, 072304 (2003).
18. K. Adcox *et al.* Phys. Rev. Lett.**88**, 022031(2002)and S. S. Adler et al. Phys. Rev. Lett **91**, 072302 (2003).
19. B. B. Back *et al.* nucl-ex/0302015 and Phys. Rev. Lett **91**, 072302 (2003).
20. C. Albajar *et al.* Nucl. Phys. **B355** 261 (1990).
21. J.Adams *et al.*, nucl-ex/0305015.
22. M. M. Aggarwal *et al.*, Eur. Phys. J. **C18** 651 (2001).
23. H. Appelshauser *et al.*, Phys. Rev. Lett. **82** 2471 (1999).
24. G. Agakishiev *et al.*, hep-ex/0003012.
25. X. N. Wang and M. Gyulassy, Phys. Rev. Lett. **68**,1480(1992).
26. M. Gyulassy and M. Plümer, Phys. Lett.**B243**, 432 (1990).
27. D. Kharzeev, E. Levin, L. McLerran, Phys. Lett. **B561** (2003) 93.
28. J. W. Cronin *et al.*, Phys. Rev. **D11** 3105 (1975).
29. I. Vitev, Phys. Lett. **B562**, 36 (2003) and M. Gyulassy *et al.* nucl-th/0302077.
30. K. Gallmeister, C. Greiner, Z. Xu, Phys. Rev. C**67** (2003) 044905.